Chapter for Methods in Molecular Biology

Edited by A. Fenton, Humana Press Inc., Totawa, NJ

Allosteric Coupling Between a Protein's Metal Binding Sites

Nicholas E. Grossoehme[1,2] and David P. Giedroc[1]

[1]Department of Chemistry, Indiana University, Bloomington, IN 47405-7102 USA

[2]Department of Chemistry, Physics and Geology, Winthrop University, Rock Hill, SC 29733, USA

Abstract

Intracellular concentrations of metal ions are controlled at the transcriptional level by a variety of metalloregulatory proteins that respond to non-homeostatic metal concentrations to elicit the appropriate cellular response, *i.e.* upregulation of genes coding for metal export or detoxification. These proteins are a specialized class of allosteric regulators that tend to be ideal for studying allostery on a grand scheme due to their size, stability, reactivity and the spectroscopic properties of metal ions, the allosteric triggers. In addition to the commonly studied heterotropic communication between metal binding and DNA affinity, many of these proteins are also characterized by homotropic allostery; communication between two or more identical metal binding sites. This chapter aims to guide the reader through the design and execution of experiments that quantify the thermodynamic driving forces (ΔG_C, ΔH_C and ΔS_C) that govern the degree to which homotropic and heterotropic allosteric interactions influence the behavior of the protein as well as guide the reader through the steps necessary for removing complex speciation from the experimental values.

1. Introduction

Allostery is the simple idea that binding of an effector molecule can influence the chemistry or reactivity at another, often spatially distinct, site(*2*). This communication has evolved as a necessary feature of a wide variety of biological macromolecules and is essential for proper cellular function. Cellular sensory machinery, for example transcriptional regulatory proteins, takes advantage of this phenomenon by enabling communication between an effector binding site and a DNA binding interface such that population of the effector site influences the affinity of the protein for its DNA binding partner; this is an essential feature of life. While other chapters in this book focus on many facets of measuring allostery, ranging from specific techniques to mapping the communication pathway, this chapter focuses on a general technique to quantify the thermodynamic forces that govern communication between one binding site and another. We specifically focus on metalloregulatory proteins, a specialized class of allosteric transcriptional regulators, which are characterized by many features that make the proteins ideal models for understanding allosteric communication(*4*). Further, these proteins, like other classes of transcriptional regulators, provide an opportunity to observe two types of allosteric communication; heterotropic, which is the communication between the regulatory site and the DNA binding interface, and homotropic, which derives from the observation that identical metal binding sites are characterized by different thermodynamic properties.

1.1 Heterotropic Allosteric Coupling

The widely accepted and applied model of allostery(*5*) that will be drawn upon for this review is depicted in **Fig. 1**. This model is characterized by closed thermodynamic cycle ($\sum_{i=1}^{4} \Delta X_i = 0$, where X is any thermodynamic state function) with the four corners occupied by the four theoretical states that a protein can adopt. When the allosteric protein is a metalloregulator, these are the apoprotein,P, the fully metal coordinated protein, PM, a DNA associated state, PD, and the ternary complex, PMD, where the protein is coordinated by metal and DNA. The magnitude of the equilibrium constants that describes the transition between these four states dictates the biological role of a metalloregulator. For example, if $K_4 >> K_3$, the PMD and P states are stable in solution and the protein is likely responsible for regulating metal uptake pathways. Alternatively, in cases that $K_3 >> K_4$, the PM and PD states are biologically relevant and the regulator is probably involved in controlling the levels of metal efflux or detoxification machinery(*6-8*).

This scheme provides a general means to determine the degree to which an affector molecule can influence the protein's affinity for DNA, that is, measure the extent to which a protein allosterically couples two distinct sites. When considering the brief discussion above that compared the protein-DNA affinities, it can be concluded that this coupling energy must be related to the relative magnitudes of these two equilibrium constants. Indeed, the coupling energy is extracted from the ratio

$$K_C = \frac{K_4}{K_3} = \frac{K_2}{K_1} = \frac{[P][PMD]}{[PD][PM]} \qquad (1)$$

and describes the ligand exchange equilibrium

$$PM + PD \rightleftharpoons P + PMD \quad (2)$$

This is perfectly consistent with the example given just above; when $K_4 >> K_3$, the products of Eq. 2 will be favored. As Eq. 1 shows, this comparison can also be made between the overall metal binding equilibria, K_1 and K_2, which suggests that quantifying the allosteric coupling between metal binding and DNA binding can be accomplished if either pair of equilibria (vertical/red or horizontal/blue boxes in **Fig. 1**) can be measured. It then follows that the coupling free energy, ΔG_C, is simply calculated from the thermodynamic relationship in Eq. 3 and can be further described according to other fundamental thermodynamic relationships (Eq. 4-5).

$$\Delta G_C = -RT \ln K_C \quad (3)$$

$$\Delta H_C = \Delta H_4 - \Delta H_3 = \Delta H_2 - \Delta H_1 \quad (4)$$

$$\Delta S_C = \Delta S_4 - \Delta S_3 = \Delta S_2 - \Delta S_1 \quad (5)$$

However, this cycle is complicated by multiple metal binding events for many metalloregulators. The cycle in **Fig 1** therefore needs to be extended to include these additional equilibria, as shown in **Fig 2**. Note that the two individual allosteric cycles, corresponding to the first and second metal binding events, are highlighted by the green and orange boxes, respectively. It is also notable that if the two sequential metal binding events are considered a single overall event, then the cycle collapses to that described in **Fig 1,** (see **Note 1**). Calculating the allosteric energies for the individual cycles (green and orange boxes in **Fig. 2**) can be accomplished exactly as described for the simplified example above, however the addition equilibria must be included for the overall cycle in **Fig. 2**

$$K_C = \frac{K_{DNA3}}{K_{DNA1}} = \frac{\beta_{MD2}}{\beta_{M2}} = \frac{[P][PM_2D]}{[PD][PM_2]} \quad (6)$$

where K_C describes the ligand exchange reaction

$$PM_2 + PD \rightleftharpoons P + PM_2D \quad (7)$$

and the coupling enthalpy and entropy are calculated with

$$\Delta H_C = \Delta H_{DNA3} - \Delta H_{DNA1} = (\Delta H_{MD1} + \Delta H_{MD2}) - (\Delta H_{M1} + \Delta H_{M2}) \quad (8)$$

$$\Delta S_C = \Delta S_{DNA3} - \Delta S_{DNA1} = (\Delta S_{MD1} + \Delta S_{MD2}) - (\Delta S_{M1} + \Delta S_{M2}) \quad (9)$$

1.2 Homotropic Allosteric Coupling

Homotropic allostery in transcriptional regulators is specific to proteins, typically homodimeric, that contain at least two identical affector binding sites. If the binding of the first ligand influences the thermodynamic properties of the second binding event, then this system exemplifies homotropic allostery. Measuring this form of allostery is particularly convenient since it can be observed in a single metal binding experiment as can be seen in the representative titration in **Fig 3**. **Fig. 4**, which depicts the scheme in which two metal ions, M_1 and M_2, bind to a protein with homotropic allosteric communication, demonstrates that the two metal association events are not statistically equivalent. It is therefore necessary to correct the macroscopic binding constants, K_{M1} and K_{M2}, determined from standard fitting procedures. This is accomplished by casting the binding events in terms of a single microscopic event, *k*, and a cooperativity term, ω, as demonstrated in Eqs 10-12(*9*).

$$K_{M1} = 2k \tag{10}$$

$$K_{M2} = \frac{\omega k}{2} \tag{11}$$

$$\Delta G_C = -RT \ln \omega = -RT \ln \frac{4K_{M2}}{K_{M1}} \tag{12}$$

According to this analysis, ω is the microscopic coupling constant and its magnitude dictates the degree to which two homotropic binding events are coupled. When ω >1, the binding of the first ligand increases the affinity of the 2nd ligand (positively cooperative) and, conversely, when ω < 1, the system is characterized by negative cooperativity. The enthalpic and entropic coupling energies can be calculated from Eqs 13 and 14, respectively.

$$\Delta H_C = \Delta H_{M2} - \Delta H_{M1} \tag{13}$$

$$\Delta S_C = \frac{-\Delta G_C + \Delta H_C}{T} \tag{14}$$

2. Materials

1. The ultimate goal of the research described here is to quantify the global thermodynamics that drive allosteric processes. Therefore, a sensitive microcalorimeter is necessary. Two common commercial sources for this instrument are MicroCal, LLC. (Northampton, MA) and TA Instruments (New Castle, DE), respectively. In addition to the standard 1.4 or 1 mL reaction cell volumes, each of these suppliers also offer a more contemporary model that minimizes sample volume (~200 μL) and increases absolute sensitivity(*10*) (see **Note 2**)
2. Reagents of the highest purity are strongly recommended since even modest contamination can significantly influence the solution properties of metal ions. High

purity standard biological reagents (buffers, etc.) are typically available from a variety of suppliers (*e.g.* Sigma, Fisher, VWR). Most metal salts are available in ultra high purity grade from Alfa Aesar.

3. If anaerobic conditions are necessary, appropriate oxygen free chambers are necessary for sample preparation and calorimetric measurement.
4. DNA binding and metal into protein/DNA complex titrations requires duplex DNA corresponding to the native operator sequence. Single stranded DNA oligonucleotides are commercially available in high purity from a number of commercial sources including Operon (Huntsville, AL) and IDT (Coralville, IA). Following purification (see **Note 3**), accurately determine ssDNA concentration using the appropriate extinction coefficient (http://www.idtdna.com/analyzer/Applications/OligoAnalyzer/). Anneal the two strands by mixing equimolar concentrations in an eppindorf tube and heating to 95 ˚C followed by slowly cooling to room temperature, with DNA duplex formation confirmed by native polyacrylamide gel electrophoresis. Care must be taken to avoid fold-back intramolecular DNA hairpin structures that might arise from the palindromic or self-complementary nature of the individual ssDNA strands (see **Note 4**). DNA duplexes prepared in this way are stored at –20 ºC and are stable indefinitely.
5. Protein preparation should be carried out by standard protocols [see **Note 5**]. It is recommended that samples estimated to be ≥ 95% pure by SDS-PAGE are used.

3. Methods

3.1. Solution condition considerations

Conditional variability can appreciably influence the heat measured by bulk thermodynamic techniques such as ITC. It is therefore of paramount importance to select

appropriate solution conditions. Listed below are a number of conditional variables that should be specifically addressed. Note that this is not an exhaustive list and additional considerations should be identified on an individual experiment basis. In general, it is recommended to select solution conditions that generate identifiable speciation that will enable robust mathematical interpretation.

1. *pH.* In addition to the obvious effects of pH on biological macromolecules (*i.e.* acid/base catalyzed hydrolysis), pH can significantly influence the solution properties of cationic metals. For example, at basic or neutral pH, Fe^{3+} is sparsely soluble ($K_{sp} = 2.64 \times 10^{-39}$) (*11*) The ideal pH would mimic the conditions that dictate the chemistry *in vivo*. Note that the pH can significantly influence the apparent affinity as will be discussed later.
2. *Buffer.* The obvious criterions for buffer selection is to maintain a constant pH, however when metal ions are of interest, the metal-buffer interactions must be considered since nearly all buffers associate with metal ions to some degree(*12, 13*), although a number of these are very weakly coordinating(*14*). It is also notable that some buffers promote redox activity through stabilization of one oxidation state relative to another (*e.i.* copper(*15*)). As noted above, it is recommended that buffers which generate a robust metal-buffer interactions are chosen to limit unquantifiable metal solution chemistry. A number of resources are available to guide the reader to buffers with metal chemistries rigorously quantified(*12, 13*). If the experiment necessitates a specific buffer and thermodynamic information is not available for this system, these values may be determined calorimetrically using the guidelines provided below(*1, 16-18*). Some experiments will require the presence of a strong metal chelator to enable measurement

of a quantifiable binding curve (*vida infra*); in these cases the metal-buffer interaction may be insignificant.

3. *Ionic Strength.* The ionic strength (*I*) of a solution directly influences the activity coefficient, and hence the measurable equilibrium constant. Eq. 15 shows Debye-Hückel relationship which indicates that *I* is a function of the total ionic content and scales with the square of the valency (z_i) for each species (i).

$$I = \frac{1}{2}\sum_i z_i^2 [i] \qquad (15)$$

In theory, all ions in solution should be included in this calculation, however under typical experimental conditions (50-500 mM monovalent salt concentration [see **Note 6**]), the contribution from metal salts and macromolecule are negligible, although it may be necessary to consider the influence of the buffer at elevated concentrations. 100 mM monovalent salt has commonly been used for metal binding experiments (*13*) and provides a standard for direct comparisons between different systems.

4. *Temperature.* Equilibrium constants are inherently temperature-dependent and most biological processes are characterized by $\Delta Cp \neq 0$ resulting in ΔH variance with temperature. Since K and ΔH are the two directly measureable variables in an ITC experiment, temperature is an important variable to consider. Fortunately, modern calorimeters maintain a constant experimental temperature (~4-80 ºC) over the course of very long experiments. Therefore, researchers need only to decide the most appropriate temperature for the system of interest. 25º C and 37º C have been commonly used.

5. *Oxygen Sensitivity.* Due to the largely reducing potential of most intracellular environments, metal ions and surface cysteines tend to be in a reduced state, *i.e.* Cu^{+} and Cys-SH or Cys-S^{-} as compared to Cu^{2+} and Cys-S–S-Cys. For systems that are

susceptible to oxidation, anaerobic preparation and experimentation is strongly advised. The application of 'pseudo-anaerobic' conditions is an error-prone approach for multiple reasons. Primarily, under these conditions, a reducing agent is absolutely necessary to maintain the appropriate redox state of reactants; most common reducing agents interact with metal ions significantly, with dithiothreitol (DTT) being the most dramatic case as many metal ions make very high affinity metal-DTT complexes (*13, 19*). These complexes will likely out-compete the desired metal-protein interactions, particularly in light of the the large excess that will be necessary for these experiments. Further, extensive control experiments will be needed to verify that the unavoidable redox chemistry (reducing agent oxidation) is not influencing the net heat flow (the direct source of data). For these reasons, it is strongly advised that oxygen sensitive experiments be conducted under strictly anaerobic conditions (see **Section 3.3**).

3.2. Metal-free Buffers

As this guide is geared towards quantifying metal ion driven chemistries, it is necessary to ensure that all materials are prepared in a way to minimize contamination. For systems not focusing on metals, the guidelines below are still worthwhile as they will ensure minimal interference from extraneous sources.

1 *Preparation of Glassware.* Standard silicate laboratory glassware is very susceptible to metal contamination. This is particularly true for 'hard' metals (*i.e.* Fe^{3+} and Mg^{2+}) which form strong electrostatic interactions with anions(*20*). Metalloregulatory proteins, which can possess very high affinities for their cognate metal(*21, 22*), can therefore leach metals from contaminated glass surfaces., and thus can potentially "leach" metals from

contaminated surfaces. This is easily avoided by ensuring that all glassware is soaked in 1% nitric acid (HNO_3) enabling protons to out-compete metal ions at the surface. Following acid treatment, the glassware should be rinsed exhaustively (≥3 times) with metal-free water (see below) to avoid an unwanted change in the pH buffer solutions.

2. *Metal Free Water.* Standard RODI water purification, common in most research laboratories, is not sufficient to remove metal ions to the degree required for quantitative metal binding experiments. Further purification can be provided by numerous standard purification systems that are capable of deionization to a resistance ≥ 18 MΩ-cm. Alternatively, strong metal chelators conjugated to solid styrene beads are commercially available, *i.e.* Chelex, and can be used to treat laboratory grade RODI water in order to produce operationally defined "metal-free" water. This can be accomplished by passing water through a vertical column containing chelating resin and collect in an acid washed container. Alternatively, the resin can be added directly into the water and shaken for several hours. Incubation at elevated temperatures can expedite this procedure. Separate the phases by centrifugation and careful decanting.
3. *Buffer Preparation.* Buffer salts, as provided by the manufacturer, are commonly contaminated with small amounts of divalent metal ions. Removal of metal ions can easily be accomplished by treating the prepared buffer with Chelex, as described just above. Note that Na^+ or H^+ ions (depending on the regeneration protocol used for the Chelex resin) will replace the metals to maintain electrostatic neutrality and, depending on the amount of metal removed from the buffer, this may be significant. pH and conductivity measurements of the post-Chelex solution is strongly suggested.

3.3. Anaerobic Preparations

For cases that require extra care to minimize oxidative conditions as discussed in **Section 3.1**, additional steps must be taken to ensure a rigorously anaerobic environment since thoroughly deoxygenated buffers and solutions are required by these experiments.

1. Prepare the buffer solution using metal-free water and remove residual metal as necessary (see **Section 3.2**).
2. Two standard degassing protocols are available to ensure all solvents are free of oxygen. The first method is a more rapid, however has the potential for mild increase in salt and buffer concentration due to water evaporation (see **Note 7**) while the second is much more thorough and minimizes solvent evaporation (see **Note 8).**
3. Stock metal solutions should be prepared and stored under an inert atmosphere. The simplest method is to dissolve a known mass of metal salt in an anaerobic chamber (Vacuum Atmospheres or Coy). If an anaerobic chamber is not available, deoxygenation can be accomplished sub-optimally by extensive bubbling of argon or nitrogen from a cylinder of compressed gas through a metal stock solution. The concentration of this stock solution should be verified by standard metal quantification techniques prior to use.
4. Completely buffer exchange the purified protein into an oxygen-free buffer. Concentrate the protein stock to ~1-2 mL, transfer to an anaerobic chamber and dialyze at least 4 h in 500 mL of the buffer to be used to metal binding experiments. The dialysis buffer should be exchanged four times to ensure complete removal of metal chelators and reducing agents that may have been used during protein purification.

3.4. Metal Binding Assays

In general, many experimental design considerations are discussed in detail in instrument manuals(*23*), and any user should be familiar with these publications. It is recommended that titrations are designed that involve well-defined metal-chelator interactions as direct titrations involving 'free' metal ions pose a number of potential problems. As mentioned above, unknown solution chemistry may be occurring that cannot be appropriately accounted for. Further, it is highly unlikely that metal ions are present in a cellular environment not associated with a cellular chelator. Secondly, it is quite likely that a direct titration of metal → protein lies outside of the experimental window that allows for a robust fit to a unique binding constant. An example titration of Zn^{2+} into CzrA, a homodimeric Zn^{2+}/Co^{2+} sensor from *Staphylococcus aureus*, is shown in **Fig. 3**.

1 Ensure the calorimeter is well maintained, calibrated, and operating properly, Refer to the instrument manual for specific directions.

2 Prepare at least 2 mL of 10 - 100 μM protein in a predetermined experimental buffer. Ensure the buffer is metal free as described in **Section 3.2**. At least four rounds of dialysis are recommended. The dialysis buffer from the last round should be saved to prepare the metal solution and used in the reference cell of the calorimeter.

3 Prepare at least 1 mL of 1 mM (see **Note 9**) metal salt from a stock solution (see **Note 10**) in the appropriate experimental buffer. It has been our experience that preparing extra (~10 mL) metal titrant solution is ideal because it enables concentration determination (via AAS or ICP-MS) of this solution eliminating error arising from dilution. To ensure that the buffer exactly matches the protein buffer, the buffer from the final protein dialysis step may be used.

4 Ensure that the calorimeter has been thoroughly cleaned (see **Note 11**).

5 Rinse the sample cell and titration syringe with the experimental buffer.

6 Load the titration syringe, sample cell, and reference per manufacturer's recommendations.

7 Insert the appropriate experimental parameters. This may be a trial and error process to determine the ideal values. While the experiment is running, pay close attention to the injection volumes, as large injections may mask data inflections and make fitting impossible or inaccurate (see **Note 12**). If the instrument cycle is complete before the reaction has reached completion, it may be possible to refill the syringe and continue the experiment (this can be done multiple times if necessary, refer to instrument specifications). Once all data is collected, the files can be concatenated. MicroCal has developed a software to automate this procedure.

8 Repeat the experiment at least two more times. Make appropriate adjustments to the experimental parameters.

If the goal is to quantify the heterotropic coupling energy, this set of experiments must be repeated in the presence of DNA. Duplex DNA preparation is described in the Materials section. Note that depending on the relative affinities, this measurement may be very challenging unless very high concentrations can be reached (see **Note 13**). It is strongly urged that complex integrity be evaluated after the completion of the experiment(*1*).

1 Select a gel filtration column capable of separating dsDNA and the metal-bound or apo protein complex from the protein-DNA complex. Pass each of these solutions across the column to generate a retention volume profile for the system of interest.

2 Collect the contents of the reaction cell once the reaction has reached completion. Take all necessary precautions regarding specific techniques necessary for the system (*i.e.* anaerobic).

3 Load the sample on the calibrated gel filtration column, making sure to monitor the absorbance at 260 nm and 280 nm. If the protein of interest has a low molar extinction coefficient, monitor at 240 nm as well.

4 Collect the appropriate fractions.

5 Quantify the total metal concentration contained in these two samples.

6 Calculate the total metal-protein stoichiometry for the two samples. Make sure to account for dilution.

3.5 Accounting for Speciation

3.5.1 Adjusting the Binding Constant

Metal speciation is unavoidable under the solution conditions necessary to conduct these experiments and standard data fitting packages currently cannot interpret such complicated equilibria. It is therefore necessary to deconvolute the thermodynamic values generated by fitting the experimental data to standard physical models. However, as mentioned above, if the experiment is carefully designed, all interactions will be known and can be accounted for using the simple approach described here. For the purpose of this exercise, it is assumed that two metal-buffer species are generated, MB and MB_2, where B is the form of the buffer that interacts with the metal ion, likely the deprotonated form and L, the macromolecule of interest, is present as a single species. Note that the 'buffer' can be any metal chelator (*ie* NTA) in solution. This approach can easily be extended to more complicated systems, such

as relevant ligand protonation chemistry, which is very likely due to the biological pH values (see **Note 14**).

$$(1-\alpha_{MB}-\alpha_{MB2})\mathrm{M} + \alpha_{MB}\mathrm{MB} + \alpha_{MB2}\mathrm{MB_2} + \mathrm{L} \rightleftarrows \mathrm{ML} + (\alpha_{MB}+2\alpha_{MB2})\mathrm{B} \quad (16)$$

In this expression, α_{MB} and α_{MB2} are the stoichiometric coefficients associated with MB and MB_2, respectively, and determined from the individual equilibrium constants [see **Notes 1 and 15**].

$$\alpha_{MB} = \frac{[MB]}{C_M} = \frac{K_{MB}[B]}{\alpha_{Buffer}} \quad (17)$$

$$\alpha_{MB2} = \frac{[MB]}{C_M} = \frac{\beta_{MB2}[B]^2}{\alpha_{Buffer}} \quad (18)$$

$$\alpha_{Buffer} = 1 + K_{MB}[B] + \beta_{MB2}[B]^2 \quad (19)$$

The standard *one-site* fitting model assumes a direct interaction between species according to

$$\mathrm{M} + \mathrm{L} \rightleftharpoons \mathrm{ML} \quad (20)$$

$$K_{ITC} = \frac{[ML]}{[M][L]} \quad (21)$$

This assumption ensures that all metal ions are present as the free metal (M) or associated with the ligand such that

$$K_{ITC} = \frac{[ML]}{(C_M - [ML])(C_L - [ML])} = \frac{[ML]}{[M][L]} \quad (22)$$

where C_M and C_L are the total metal and ligand concentrations, respectively. This, of course, is not the case for the chemical system described by eq. 16. Therefore, eq. 22 must be adjusted to account for the additional chemical species present in the reaction.

$$K_{ITC} = \frac{[ML]}{(C_M - [ML])(C_L - [ML])} = \frac{[ML]}{(1 + K_{MB}[B] + \beta_{MB2}[B]^2)[M][L]} = \frac{K_{ML}}{\alpha_{Buffer}} \tag{23}$$

It then follows that the apparent binding constant, K_{ITC}, can be converted to the buffer-independent value, K_{ML}, by simply multiplying it by the metal-buffer reaction quotient, α_{Buffer}. If it is necessary to account for acid-base equilibria, a similar competition value may be added to the expression (see **Note 14**).

3.5.2 Adjusting the Enthalpy

To extract the enthalpy associated with metal-protein interactions and the corresponding protein structural or dynamic response (Eq. 20), additional heats associated with unavoidable coupled chemical events must be subtracted from the overall measured enthalpy, $\Delta H_{overall}$. To accomplish this, Hess' Law is applied to the overall equilibrium which enables the isolation of individual equilibria that contribute to the net heat. For this example, we will extend the equilibrium in Eq. 16 to include a single protonation event on the ligand since subtraction of proton-buffer heats is essential.

$$(1-\alpha_{MB} - \alpha_{MB2})\mathrm{M} + \alpha_{MB}\mathrm{MB} + \alpha_{MB2}\mathrm{MB_2} + (1-\alpha_{HL})\mathrm{L} + \alpha_{HL}\mathrm{HL} \rightleftarrows$$

$$\mathrm{ML} + (\alpha_{MB}+2\alpha_{MB2}- \alpha_{HL})\mathrm{B} + \alpha_{HL}\mathrm{HB} \tag{24}$$

$$\alpha_{HL} = \frac{[HL]}{C_L} = \frac{K_{HL}[H]}{\alpha_{Proton}} \tag{25}$$

$$\alpha_{\mathrm{Pr}oton} = 1 + K_{HL}[H] \tag{26}$$

To begin Eq. 24 disassembly, we will identify three categories of equilibria; those involving metal-buffer interactions (Eqs. 27-28), those involving proton flow (Eqs. 29-30), and the desired metal-ligand interaction (Eq. 31). Note that the equations are written such that they sum up to the overall equilibrium and Eq. 27 – 29 are the reverse of the association reaction, therefore a negative sign must be placed in front of standard state functions to describe the equations as written.

$$\{MB \rightleftharpoons M + B\}\ \alpha_{MB} \tag{27}$$

$$\{MB_2 \rightleftharpoons M + 2B\}\ \alpha_{MB2} \tag{28}$$

$$\{HL \rightleftharpoons L + H\}\ \alpha_{HL} \qquad -\alpha_{HL}\Delta H_{HL} \tag{29}$$

$$\{B + H \rightleftharpoons HB\}\ \alpha_{HL} \qquad \alpha_{HL}\Delta H_{HB} \tag{30}$$

$$M + L \rightleftharpoons ML \tag{31}$$

According to this scheme, the heat associated with Eq. 31 (ΔH_{ML}) can be calculated by subtracting the heat from Eq. 27 through Eq. 30 ($-\alpha_{MB}\Delta H_{MB,}$ $-\alpha_{MB2}\Delta H_{MB2,}$ - $\alpha_{HL}\Delta H_{HL,}$ and α_{HL} H_{HB}, respectively) from the $\Delta H_{overall}$. This necessitates prior knowledge of all these values. While this is reasonable for ΔH_{HB} from literature sources, the specific set of conditions will influence the other equilibria. Therefore, it is necessary to experimentally determine each of these. This protocol exploits the well characterized metal-EDTA interactions(*13*) to determine the total metal-buffer heat ($\Delta H_{MBtot} = -(\alpha_{MB}\Delta H_{MB} + \alpha_{MB2}\Delta H_{MB2})$).

1 Ensure the cleanliness and proper operation of the calorimeter (see **Note 11**).

2 Prepare at least 2 mL of 100 μM (see **Note 10**) EDTA in an identical buffer used for the metal-protein titration.

3 Prepare at least 1 mL of 1 mM (see **Note 9**) metal salt in identical experimental buffer.

4 Conduct the titration using the appropriate instrument settings. It is recommended to use the same settings as the metal-protein titration.

5 Repeat at least twice.

6 Average the measured heats. Propagate error appropriately(*24*).

7 Calculate α_{HL} and α_{H2L}, and α_{Proton} (see **Note 16**) from $K_{HL} = 10^{9.52}$ and $\beta_{H2L} = 10^{15.65}$.

8 Calculate ΔH_{MBtot} according to

$$\Delta H_{MBtot} = \Delta H_{overall} - \alpha_{HL}(\Delta H_{HB} - \Delta H_{HL}) - \Delta H_{ML} \quad (32)$$

This value can then be used to subtract ΔH_{MBtot} from any reaction under identical conditions. Further, this set of equations and approach is completely generic and can be applied to any metal-ligand interaction assuming that adjustments are made in each category for additional (or fewer) species.

3.5.3 Determining Protons Displaced Calorimetrically

As described above, due to the dramatic influence buffer-proton interactions can have on the overall ΔH, it is necessary to subtract this value from $\Delta H_{overall}$. To accomplish this correctly, the number of protons (n_{H+}) must be known. If all relevant pK_as are known, this value can easily be calculated according to Eq. 29, however for biological macromolecules, it is likely that it will need to be experimentally determined.

$$n_{H+} = \sum_i i\alpha_{HiL} \quad (33)$$

While this can be accomplished by other methods(*25*), determining this value calorimetrically provides additional thermodynamic data and makes the overall values more statistically robust. This method(*26, 27*) draws on the fact that, under identical conditions, changing the buffer will only lead to a change in the heat associated with the buffer chemistry; for the case at hand, this includes metal-buffer and proton-buffer interactions.

1 Select a buffer that enables robust pH buffering at the experimental pH, however has a significantly different $\Delta H_{Hbuffer}$ as determined from literature sources(*13*).

2 Prepare the protein and buffer taking the necessary steps to ensure otherwise identical experimental conditions (*i.e.* ionic strength, pH) and ideally using the same batch of protein stock.

3 Conduct metal → chelator titrations in this new buffer, to enable subtraction of metal-buffer interactions, as described in **Section 3.5.2**. Note that some metal-buffer pairs can influence the ligand exchange kinetics, therefore keenly monitor the first few injections as well as the injections nearing stoichiometric equivalence (see **Note 12**).

4 Conduct metal → protein titrations in triplicate in the new experimental buffer, taking care to ensure that the same experimental temperature, and making sure to monitor the appropriate injections (see **Note 12**).

5 Repeat this procedure with more buffers as needed.

Once the data is collected and the metal-buffer interactions are subtracted, plotting $\Delta H_{Hbuffer}$ *vs.* ΔH_{ITC} will generate a straight line with the slope corresponding to the number of protons displaced (or consumed), n_{H+}, under this specific set of experimental conditions, according to

$$\Delta H_{ITC} = n_{H+}\Delta H_{HBuffer} + \Delta H_{ML} \quad (34)$$

where ΔH_{ML} is the heat associated with the metal-protein interaction.

4. Notes

1. Standard equilibrium nomenclature defines β as an overall binding constant and is therefore the product of sequential equilibrium constants ($\beta_{MB2} = K_{MB}K_{MB2}$). Ensure that the equilibrium constants used for these calculation describe the association equilibria ($X + Y \rightleftharpoons XY;\ K = \frac{[XY]}{[X][Y]}$).
2. For simplicity and clarity, the terminology described in the MicroCal, LLC VP-ITC user manual(*23*) will used when possible. This nomenclature indicates that the molecule in the injection syringe will be referred to as the ligand and the molecule in the reaction cell will be designated the macromolecule. However, **Section 3.5** describes the mathematical detail needed to subtract speciation from common fitting models; to remain consistent with common speciation nomenclature, M refers to the metal ion and L refers to any ligand that binds to the metal. This nomenclature is consistent with the commonly termed 'reverse' direction, which would place the metal ion in the reaction cell and the protein in the syringe.
3. Large quantities of DNA are needed for these experiments, particularly if the standard 1 or 1.4 mL reaction volumes are needed for the nanoITC (TA) or VP-ITC (MicroCal), respectively. Several 1 μM scale DNA syntheses are likely needed to generate adequate material for these experiments. We routinely further purify DNAs by denaturing PAGE followed by electroelution (l>20 nts) or high resolution anion exchange chromatography (l≤20 nts), and ethanol precipitation. In the case of denaturing PAGE-purified DNAs,

complete removal of acrylamide and urea is ensured by a final reverse phase clean up step using prepacked C18 columns (Alltech) and elution with 50% methanol. Dry to completeness with a speedvac.

4. Some duplex DNA operator sequences are highly palindromic, in which case a ssDNA hairpin may be thermodynamically favored over dsDNA. Annealing under high salt concentration (0.5-1M NaCl) promotes duplex formation. Additionally, increased strand concentration may be needed to favor the intermolecular complex formation. Note that rapid cooling should be avoided as this process favors hairpin formation.
5. Since metal binding events are of particular interest, it is strongly advised that purification by His-tags is avoided. Obviously, high affinity interactions between these motifs and metal ions can convolute the desired binding events. For measurement of allosteric systems not involving metal ions, researcher discretion is advised.
6. Elevated monovalent salt concentration in these systems is often required to enhance protein solubility. Further, if the protein-DNA interactions are of interest, high salt is often needed to ensure that the affinities are within the measurable range due to the sizeable electrostatic contribution to K_a for essentially all protein-DNA interactions (*22, 28, 29*). For a direct comparison of binding affinities between different systems, the solution conditions must obviously be identical.
7. Transfer/prepare the buffer in a 2-3 L round bottomed vacuum flask (a reaction flask from Kontes works well for this purpose). Attach the flask to a dual line manifold with one dedicated vacuum line and the other attached to a cylinder of argon. Situate the flask on a magnetic stirring mechanism and stir under high vacuum for at least one hour per liter of buffer (two hours per liter is recommended). Back-fill with argon. Stir for 1 hour

per liter ensuring that the vessel is sealed. Repeat. Transfer the sealed vessel to an anaerobic chamber. Note this method will lead to a small increase in buffer concentration as a result of unavoidable solvent evaporation.

8. Prepare the buffer in a vacuum flask (typically available up to 500 mL) leaving at least 1/3 of the flask volume empty. Submerge the flask into liquid nitrogen or an isopropanol-dry ice slurry until completely frozen. While still frozen, expose to a high vacuum for 10-20 minutes. Close the flask and warm until completely melted. Submersion in tepid water can help this process; however caution is urged to avoid fracturing the glassware as a result of a rapid temperature change. Repeat this process three times followed by backfilling the flask with Argon for transfer to an anaerobic chamber.
9. The concentration can be adjusted if necessary to account for very large or small measured heats or other experimental considerations.
10. Some metals are very insoluble at elevated concentrations unless the solution is reasonably acidic. At a give pH, the soluble metal concentration can be easily calculated from solubility products(*11*). We tend to prepare >100 mM stock metal concentrations under neutral conditions if possible. Higher stock concentrations will minimize the buffer dilution that will occur upon sample preparation, however as long as >100 mM concentrations are used, this dilution is insignificant. Regularly verify the stock concentration by standard methods.
11. While several methods are available for cleaning, if there is any uncertainty in the cleanliness of the instrument, we recommend a rigorous cleaning protocol consisting of soaking the sample cell and titration syringe in 10 mM EDTA, 1 mM DTT prepared in

0.1% detergent (such as Micro-90) at 65 ºC for 4 hours followed by a thorough rinse with metal free water (1-2 L)

12. Although monitoring all injection aliquots is a good idea, it is particularly appropriate to monitor the first several injections to verify that enough time is allowed for the solution to return to baseline. Further, the injections leading up to the stoichiometric equivalence or inflection point should also be monitored due to the reduced concentration of macromolecule and resulting slower reaction. If enough time is not allowed to verify reaction equilibrium, the data is unreliable.
13. For example, if the experiment is being carried out with 50 μM protein and $K_{DNA3} = 10^6$ M^{-1}, a rough calculation indicates that nearly 15% of the ternary complex will likely dissociate to MP and D and result in very ambiguous data fitting. However, this situation is also dependent on the other equilibria in the cycle and may well be stabilized.
14. If it is desired to account for macromolecule protonation speciation, a competition term is easily derived, $\alpha_{\mathrm{Pr}\,oton} = \sum_{i=0}^{n} \beta_i [H]^i$. However, it should be noted that unless the exact pKa values can be determined, accounting for acid-base chemistry is largely an approximation. Further, while the heat associated with amino acid protonation chemisty has been quantified, these values are for the free amino acids and any local chemistry (*i.e.* charge stabilization, dielectric constant) can significantly influence these values. Therefore, accounting for the heat associated with ligand deprotonation is also very ambiguous. For this reason, this can be ignored and the results then become pH-specific(1). However, the heat associated with buffer protonation should certainly be removed (see **Section 3.5.2 and 3.5.3**)

15. It is assumed that the buffer is in large excess and the concentration is effectively constant.

$$\alpha_{\mathrm{Pr}oton} = 1 + 10^{9.52}[H] + 10^{15.65}[H]^2$$

16.
$$\alpha_{H2L} = \frac{10^{15.65}[H]^2}{\alpha_{\mathrm{Pr}oton}}$$

References

1. Grossoehme, N. E., and Giedroc, D. P. (2009) Energetics of Allosteric Negative Coupling in the Zinc Sensor S. aureus CzrA, *Journal of the American Chemical Society 131*, 17860-17870.
2. Monod, J., Wyman, J., and Changeux, J.-P. (1965) On the nature of allosteric transitions: A plausible model, *Journal of Molecular Biology 12*, 88-118.
3. Popovych, N., Sun, S., Ebright, R. H., and Kalodimos, C. G. (2006) Dynamically driven protein allostery, *Nat Struct Mol Biol 13*, 831-838.
4. Ma, Z., Jacobsen, F. E., and Giedroc, D. P. (2009) Coordination Chemistry of Bacterial Metal Transport and Sensing, *Chemical Reviews 109*, 4644-4681.
5. Reinhart, G. D., Jo M. Holt, M. L. J., and Gary, K. A. (2004) Quantitative Analysis and Interpretation of Allosteric Behavior, in *Methods in Enzymology*, pp 187-203, Academic Press.
6. Giedroc, D. P., and Arunkumar, A. I. (2007) Metal sensor proteins: nature's metalloregulated allosteric switches, *Dalton Transactions*, 3107-3120.
7. Laura S. Busenlehner, Mario A. Pennella, and David P. Giedroc. (2003) The SmtB/ArsR family of metalloregulatory transcriptional repressors: structural insights into prokaryotic metal resistance, *FEMS Microbiology Reviews 27*, 131-143.
8. Ma, Z. J., Faith E.; Giedroc, David P. (2009) Metal transporters and metal sensors: how coordination chemistry controls bacterial metal homeostasis, *Chemical Reviews in press*.
9. Lee, S., Arunkumar, A. I., Chen, X., and Giedroc, D. P. (2006) Structural Insights into Homo- and Heterotropic Allosteric Coupling in the Zinc Sensor S. aureus CzrA from Covalently Fused Dimers, *Journal of the American Chemical Society 128*, 1937-1947.
10. Peters, W. B., Frasca, V., and Brown, R. K. (2009) Recent Developments in Isothermal Titration Calorimetry Label Free Screening, *Combinatorial Chemistry & High Throughput Screening 12*, 772-790.
11. (1994) *CRC Handbook of Chemistry and Physics*, 75 ed., CRC Press, London.
12. Magyar, J. S., and Godwin, H. A. (2003) Spectropotentiometric analysis of metal binding to structural zinc-binding sites: accounting quantitatively for pH and metal ion buffering effects, *Analytical Biochemistry 320*, 39-54.
13. Technology, N. I. o. S. a. (2003) NIST Standard Reference Database 46, Version 7.0.

14. Yu, Q., Kandegedara, A., Xu, Y., and Rorabacher, D. B. (1997) Avoiding Interferences from Good's Buffers: A Contiguous Series of Noncomplexing Tertiary Amine Buffers Covering the Entire Range of pH 3-11, *Analytical Biochemistry 253*, 50-56.
15. Hegetschweiler, K., and Saltman, P. (1986) Interaction of copper(II) with N-(2-hydroxyethyl)piperazine-N'-ethanesulfonic acid (HEPES), *Inorganic Chemistry 25*, 107-109.
16. Grossoehme, N. E., Akilesh, S., Guerinot, M. L., and Wilcox, D. E. (2006) Metal-Binding Thermodynamics of the Histidine-Rich Sequence from the Metal-Transport Protein IRT1 of Arabidopsis thaliana, *Inorganic Chemistry 45*, 8500-8508.
17. Grossoehme, N. E., Mulrooney, S. B., Hausinger, R. P., and Wilcox, D. E. (2007) Thermodynamics of Ni2+, Cu2+, and Zn2+ Binding to the Urease Metallochaperone UreE&#x2020, *Biochemistry 46*, 10506-10516.
18. Grossoehme, N. E. S., Anne M.; Wilcox, Dean E. (2010) Application of Isothermal Titration Calorimetry in Bioinorganic Chemistry, *Submitted to JBIC*.
19. Krezel, A., Lesniak, W., Jezowska-Bojczuk, M., Mlynarz, P., Brasuñ, J., Kozlowski, H., and Bal, W. (2001) Coordination of heavy metals by dithiothreitol, a commonly used thiol group protectant, *Journal of Inorganic Biochemistry 84*, 77-88.
20. Cotton, A. W., Geoffrey; Murillo, Carlos A.; Bochman, Manfred. (1999) Advanced Inorganic Chemistry, 6 ed., John Wiley and Sons, New York.
21. Eicken, C., Pennella, M. A., Chen, X., Koshlap, K. M., VanZile, M. L., Sacchettini, J. C., and Giedroc, D. P. (2003) A metal-ligand-mediated intersubunit allosteric switch in related SmtB/ArsR zinc sensor proteins, *J. Mol. Biol. 333*, 683-695.
22. Ma, Z., Cowart, D. M., Scott, R. A., and Giedroc, D. P. (2009) Molecular insights into the metal selectivity of the copper(I)-sensing repressor CsoR from *Bacillus subtilis*, *Biochemistry 48*, 3325-3334.
23. MicroCal. (2002) MicroCalorimeter User's Manual, Northampton, MA.
24. Taylor, J. R. (1997) in *An Introduction to Error Analysis* 2nd ed., University Science Books.
25. Yang, X., Chen-Barrett, Y., Arosio, P., and Chasteen, N. D. (1998) Reaction Paths of Iron Oxidation and Hydrolysis in Horse Spleen and Recombinant Human Ferritinsâ€ *Biochemistry 37*, 9743-9750.
26. Doyle, M. L., Louie, G., Dal Monte, P. R., Sokoloski, T. D., and Michael L. Johnson, G. K. A. (1995) [8] Tight binding affinities determined from thermodynamic linkage to protons by titration calorimetry, in *Methods in Enzymology*, pp 183-194, Academic Press.
27. Baker, B. M., and Murphy, K. P. (1996) Evaluation of linked protonation effects in protein binding reactions using isothermal titration calorimetry, *Biophysical Journal 71*, 2049-2055.
28. Record, M. T., Jr., Ha, J. H., and Fisher, M. A. (1991) Analysis of equilibrium and kinetic measurements to determine thermodynamic origins of stability and specificity and mechanism of formation of site-specific complexes between proteins and helical DNA, *Methods in enzymology 208*, 291-343.
29. Chen, X., Agarwal, A., and Giedroc, D. P. (1998) Structural and functional heterogeneity among the zinc fingers of human MRE-binding transcription factor-1, *Biochemistry 37*, 11152-11161.

Fig. 1. Heterotropic allosteric coupling scheme. This general four-state thermodynamic cycle accounts for the possible states that a theoretical metalloregulator can adopt. The red vertical and blue horizontal boxes are the two equilibrium pairs that can be measured to determine the overall allosteric coupling energy, ΔG_C, as described in the text and the four equilibrium constants, along with concentration, dictates the population of each state.

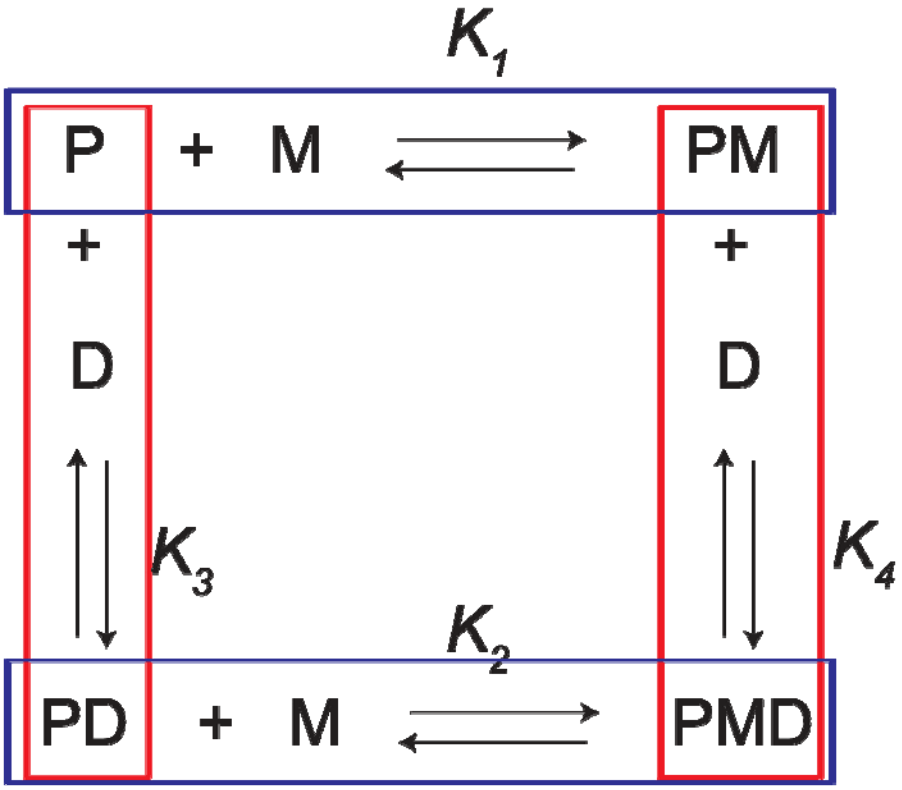

Fig. 2. Elaborated heterotropic allosteric coupling scheme. This general six-state thermodynamic cycle accounts for the four allosteric "end" states a homodimeric metalloregulatory protein (P) can hypothetically adopt apo (P), metal-bound (PM_2), DNA-bound apoprotein (PD) and a "ternary" protein-metal-DNA complex ((PM_2D). In addition, two intermediate states are shown corresponding to the singly metallated protein (PM) and 'ternary' complex (PMD). The red vertical and blue horizontal boxes are the two equilibrium pairs that can be measured to determine the overall allosteric coupling energy, ΔG_C, as described in the text. The transparent green and orange boxes highlight the thermodynamic cycles that can be used to determine the stepwise coupling energies for the individual metal ions.

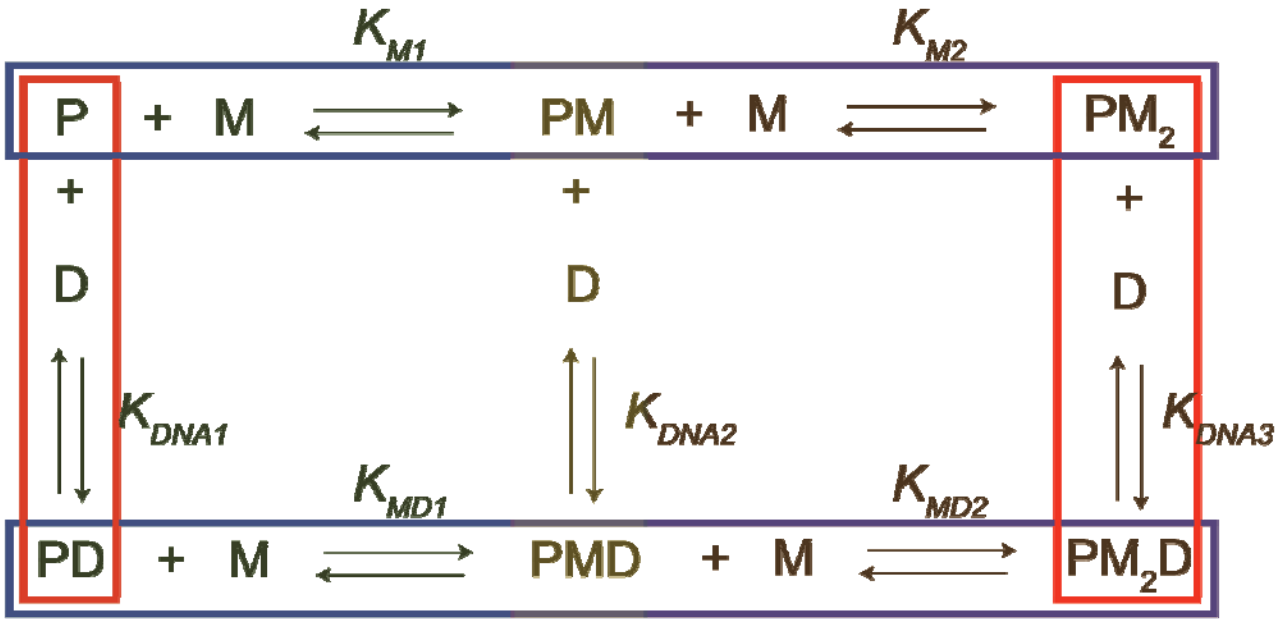

Fig. 3. Representative ITC titration exemplifying negative allosteric communication between two identical binding sites. 1.4 mM Zn^{2+} titrated into 34 µM CzrA dimer in 50 mM ACES and 400 mM NaCl at 25 ºC and pH 7.0(1). The top panel show the raw ITC data with each peak corresponding to an individual 3 µL injection (first injection is 1 µL) plotted as power vs. time. The bottom panel show the integrated, concentration normalized data plotted as ΔH vs. the Zn^{2+}-CzrA dimer molar ratio. Here we see that each CzrA dimer binds two non-equivalent Zn^{2+} ions with negative cooperativity, however this system is interestingly characterized by a homotropic coupling enthalpy, ΔH_C, that opposes ΔG_C. This feature has been observed in other allosteric regulators(*3*).

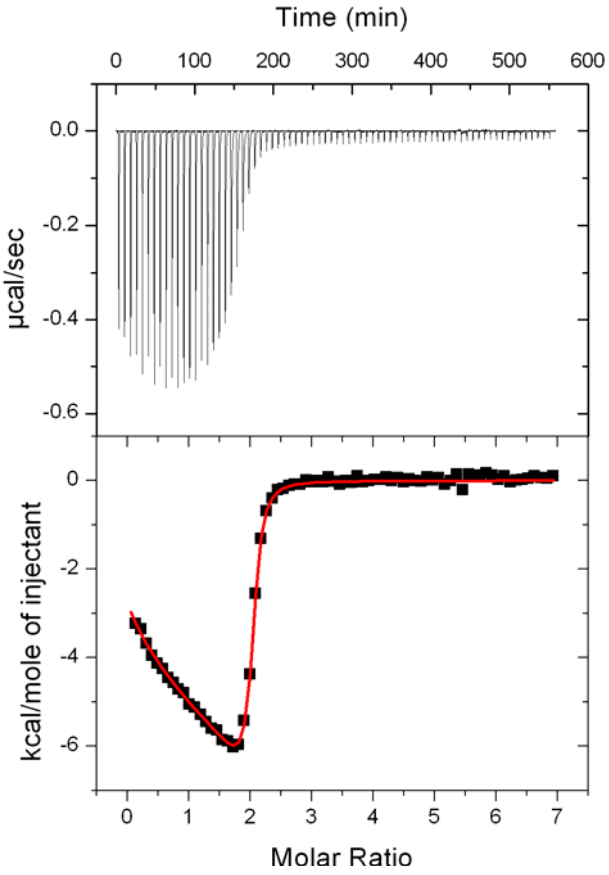

Fig. 4. Homotropic allosteric coupling scheme. This scheme depicts the chemical pathways between the three possible states for an allosteric protein. Since these are identical binding sites, they can both be described by a microscopic binding constant, *k*, which is uninfluenced by the allosteric forces that appear in the macroscopic binding constants, these forces are propagated through the cooperativity parameter, ω. Since these macroscopic constants are not equivalent, the reaction scheme indicates that a statistical treatment of the data must be included. This is described in Eq. 6-10.